Spin Chemistry Investigation of Peculiarities of Photoinduced Electron Transfer in Donor–Acceptor Linked System

I. M. Magin, N. E. Polyakov, E. A. Khramtsova, A. I. Kruppa, A. A. Stepanov, P. A. Purtov, T. V. Leshina, Yu. P. Tsentalovich, M. A. Miranda, et al.

Applied Magnetic Resonance

ISSN 0937-9347
Volume 41
Combined 2-4

Appl Magn Reson (2011) 41:205-220
DOI 10.1007/s00723-011-0288-3

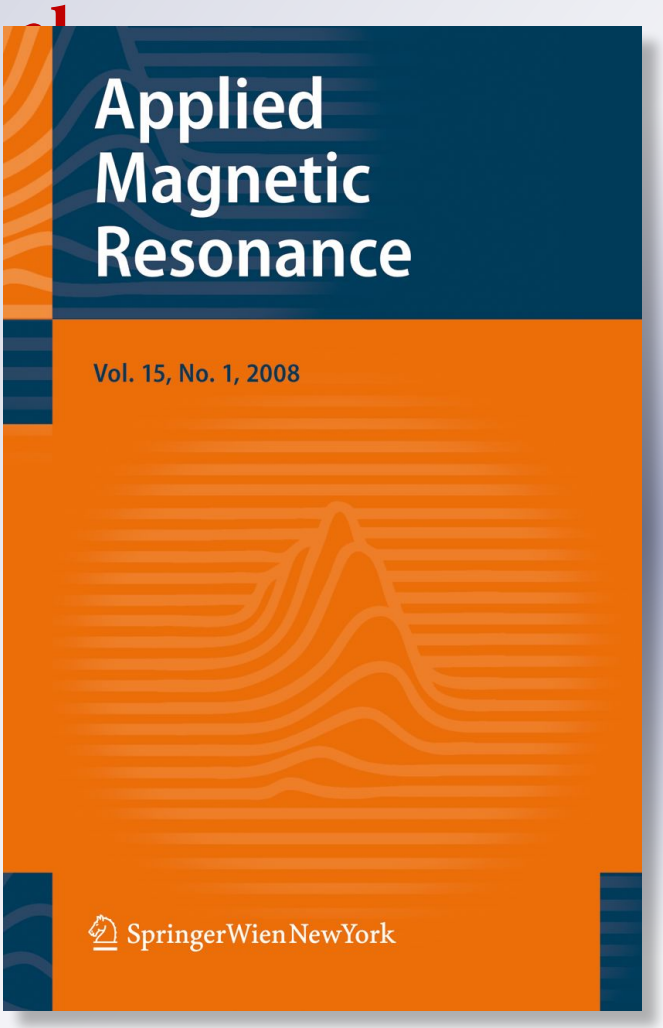

Springer

Appl Magn Reson (2011) 41:205–220
DOI 10.1007/s00723-011-0288-3

Applied Magnetic Resonance

Spin Chemistry Investigation of Peculiarities of Photoinduced Electron Transfer in Donor–Acceptor Linked System

I. M. Magin · N. E. Polyakov · E. A. Khramtsova · A. I. Kruppa · A. A. Stepanov · P. A. Purtov · T. V. Leshina · Yu. P. Tsentalovich · M. A. Miranda · E. Nuin · M. L. Marin

Received: 29 June 2011 / Revised: 14 September 2011 / Published online: 28 October 2011

Abstract Photoinduced intramolecular electron transfer in linked systems, (*R,S*)- and (*S,S*)-naproxen-*N*-methylpyrrolidine dyads, has been studied by means of spin chemistry methods [magnetic field effect and chemically induced dynamic nuclear polarization (CIDNP)]. The relative yield of the triplet state of the dyads in different magnetic field has been measured, and dependences of the high-field CIDNP of the *N*-methylpyrrolidine fragment on solvent polarity have been investigated. However, both (*S,S*)- and (*R,S*)-enantiomers demonstrate almost identical CIDNP effects for the entire range of polarity. It has been demonstrated that the main peculiarities of photoprocesses in this linked system are connected with the participation of singlet exciplex alongside with photoinduced intramolecular electron transfer in chromophore excited state quenching.

I. M. Magin (✉) · N. E. Polyakov · E. A. Khramtsova · A. I. Kruppa (✉) · A. A. Stepanov · P. A. Purtov · T. V. Leshina
Institute of Chemical Kinetics and Combustion, Siberian Branch of the Russian Academy of Sciences, Institutskaya 3, Novosibirsk 630090, Russia
e-mail: magin@kinetics.nsc.ru

A. I. Kruppa
e-mail: kruppa@kinetics.nsc.ru

E. A. Khramtsova · P. A. Purtov
Novosibirsk State University, Pirogova 2, Novosibirsk 630090, Russia

Yu. P. Tsentalovich
International Tomography Center, Siberian Branch of the Russian Academy of Sciences, Institutskaya 3-a, Novosibirsk 630090, Russia

M. A. Miranda · E. Nuin · M. L. Marin
Instituto de Tecnología Química, UPV-CSIC, Universidad Politécnica de Valencia, Av. de los Naranjos s/n, 46022 Valencia, Spain

1 Introduction

One of the elementary chemical processes, single electron transfer (SET), has been studied with undiminished interest for many years due to the presence of SET in many key processes important for chemistry and biochemistry, such as photosynthesis, reactions involving certain enzymes (oxygenase, dioxygenase, reductase, cytochromes, peroxidase, etc.), thermal and photoinduced transformations of organic compounds [1–3]. To date, a detailed study of the processes of photoinduced electron transfer (PET) has been made, in particular, the effect of such factors as the electronic structure of the donor and the acceptor, the polarity of the medium, and the excitation energy [4]. Less is known about steric factors, in particular, the effect of chiral centers present in the donor or acceptor molecular fragments. Meanwhile, the chiral systems attract special attention in recent years because of the importance of optical isomers for different areas of science, from the origin of life to pharmacological problems related to different activity of drug enantiomers [5–7].

PET processes are investigated by various techniques including laser flash photolysis, Raman spectroscopy, pulse electron paramagnetic resonance (EPR) spectroscopy, and spin chemistry [7–9]. It is worth noting that in these studies, the methods of spin chemistry occupy a special place. Using these methods, SET was proved for the first time in a number of processes, in which it had been only assumed (e.g., nucleophilic substitution reactions and sigmatropic rearrangement), or even not assumed (quenching of the excited states of aromatic donors and electron acceptors, including sensitized *cis–trans* photoisomerization) [10, 11].

In recent years, the peak of interest in studying PET processes has shifted to the so-called linked systems—molecules, which contain both donor and acceptor groups connected by rigid or flexible bridges [12, 13]. The ultimate goal of such studies is usually announced to be the design of various electronic devices and energy storage systems (light conversion systems such as photosynthetic devices). These studies may also serve as useful models for understanding the processes of electron transfer over long distances, which are postulated for several practically important enzyme systems, e.g., cytochrome–cytochrome oxidase [2]. Indeed, linked systems with different rigid or flexible spacers have proven to be good models to study the features of electron transfer processes. Note that most spin chemistry studies of linked systems (dyads and triads) were carried out using only magnetic field effects (MFE) [12, 14]. The main information obtained from the analysis of magnetic field dependence concerns the energy of the electron exchange interaction between paramagnetic centers of dyads and triads. The dyads containing aromatic chromophores like naphthalene and amine as a quencher are classic, well-studied examples of the coupled systems [15].

Recently, the difference in fluorescence quenching rate between (*R,S*)- and (*S,S*)-enantiomers of naproxen-pyrrolidine dyads (NPX-Pyr, Chart 1) has been observed. This quenching can proceed via the exciplex formation or PET, which are typical photoinduced reactions between an excited naphthalene chromophore and electron donors like amine. These two pathways should be considered as the main quenching mechanisms. Other possibilities like hydrogen transfer or energy transfer can be excluded. The electron transfer rate constants for (*S*,*S*)- and (*R*,*S*)-NPX-Pyr have

been determined in Ref. [15] from the ratio of quantum yield and fluorescence life time to be $k_e = 1.8 \times 10^8$ and 2.8×10^8 s^{-1} for (*S*,*S*)- and (*R*,*S*)-configuration, respectively.

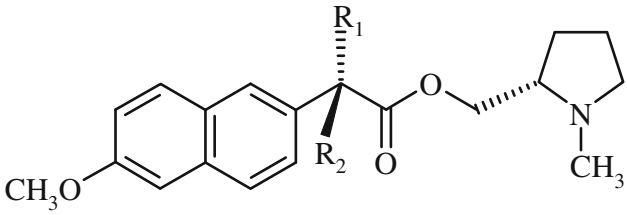

$R_1 = CH_3; R_2 = H$ (S,S)-NPX-Pyr

$R_1 = H; R_2 = CH_3$ (R,S)-NPX-Pyr

Chart 1 Structures of naproxen-pyrrolidine dyads

This is the first example of the influence of chirality on the rate of electron transfer we are aware of, although it should be noted that the difference in the rates of fluorescence quenching of various enantiomers is a reliably established fact [16]. The largest effects are obtained in nonpolar media and generally relate to processes in exciplexes [17]. Indeed, in this case one can expect a stronger influence of the spatial orientation of the partners on the efficiency of quenching. The suggestion that the main mechanism of fluorescence quenching in NPX-Pyr dyad is intramolecular PET has been made from the analysis of thermodynamics parameters of the dyads [15].

To study peculiarities of PET in linked systems, (*S*,*S*)- and (*R*,*S*)-NPX-Pyr dyads spin chemistry methods, MFE and chemically induced dynamic nuclear polarization (CIDNP), are used. In particular, we compare CIDNP effects detected in the NPX–Pyr dyad with similar results observed in related systems in solution. The systems that were selected for comparison are photoinduced interaction of naphthalene with triethylamine (TEA), methyl ester of naproxen (Me-NPX, see Chart 2) with TEA, methyl ester of naproxen with acetate of (*S*)-*N*-methyl-2-pyrrolidinemethanol (Ac-Pyr, see Chart 2).

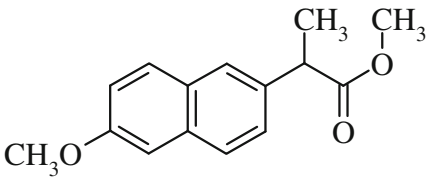

Me-NPX

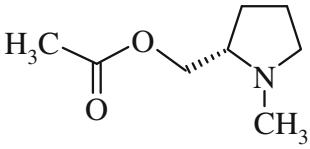

Ac-Pyr

Chart 2 Structures of methyl ester of naproxen and acetate of (*S*)-*N*-methyl-2-pyrrolidinemethanol

The first stage of this study is to establish detailed mechanisms of the processes responsible for degradation of the photoexcitation of the dyad using the two methods of spin chemistry, MFE and CIDNP. Analysis of spin polarization in this case seems quite promising, e.g., for establishing the roles of biradical ion and exciplex in quenching processes of photoexcited state of the dyad.

Quantum chemical calculations were performed using unrestricted Hartree–Fock (UHF) AM1 method (Hyperchem 7.5).

2 Experimental

The *R*,*S* and *S*,*S* naproxen-pyrrolidine dyads ((*S*)-*N*-methyl-2-pyrrolidinemethyl 2(*R*)- or 2(*S*)-(6-methoxy-2-naphthylpropanoate) and the acetate of (*S*)-*N*-methyl-2-pyrrolidinemethanol were synthesized as described earlier [16]. Methyl-6-methoxy-2-naphthylpropanoate was synthesized by the same method as described for dyads and was purified by thin-layer chromatography (TLC). 2,6-Dimethyl-naphthalene (DMN) (Aldrich) was sublimated prior to use. Triethylamine (TEA) was distilled over zinc powder. Deuteroacetonitrile (D99.9%) and deuterobenzene (D99.8%) (both by Aldrich) were used for nuclear magnetic resonance (NMR) and CIDNP experiments. Acetonitrile freshly distilled over P_2O_5 was used for MFE experiments.

^{1}H NMR spectra were recorded at room temperature on a DPX-200 Bruker NMR spectrometer (200 MHz ^{1}H operating frequency, $\tau(90) = 5.8$ μs). A Lambda Physik EMG 101 MSC eximer laser was used as the light source (308 nm, 100 mJ at output window, 20 mJ/pulse in sample volume, with pulse duration of 15 ns). For time-resolved (TR) CIDNP experiments [18, 19] the delay between the laser and detection pulses was varied from 0 to 100 μs. For CIDNP dependences on solvent polarity, the delay was set at 1 μs. Pseudo steady-state (PSS) photo-CIDNP [20] experiments were performed at room temperature. The samples in standard 5 mm Pyrex NMR tubes were irradiated directly in the probe of the NMR spectrometer at 20°C.

MFE experiments were performed using a laser flash photolysis apparatus described earlier ($\lambda_{ex} = 266$ nm; $\lambda_{obs} = 440$ nm; pulse length, 10 ns; energy, 12 mJ) [21]. MFE was monitored at 100 ns delay where the transient absorption reaches the plateau.

Dyad concentration in MFE experiments was 0.2 mM in acetonitrile. For CIDNP experiments, the concentrations of dyad, DMN and Me-NPX were 1 mM. For experiments in the presence of TEA or Ac-Pyr, their concentrations were 10 mM. A mixture of deuterobenzene and deuteroacetonitrile was used for solvent polarity variation. All samples were bubbled with argon for 15 min to remove dissolved oxygen just before photolysis.

3 Results and Discussion

According to the declared goals of this investigation, we attempt to confirm the suggestion made in Refs. [16, 22] that the main way of triplet state formation of the

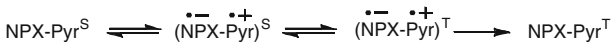

Scheme 1 Intramolecular electron transfer in NPX-Pyr dyad

NPX-Pyr dyad is singlet–triplet conversion in biradical ion—chain-linked radical ion pair (see Scheme 1).

Since the proposed way of triplet state formation includes magnetic field dependent stage, namely, singlet–triplet conversion in radical ion pair (RIP), first we have measured MFE on the yield of the triplet (see Scheme 1).

Several mechanisms of the influence of external magnetic field on the process of PET in this system can be expected. In the case of weak electron exchange interaction between the donor and acceptor fragments of the biradical ion [as compared to hyperfine interaction (HFI) constants], the usual HFI- and Δg-mechanisms must be involved in spin evolution [11]. In the case of strong electron exchange interaction, other mechanisms are possible: electron relaxation induced spin state transitions [23] and the level-crossing (J) mechanism [24]. In the latter case, the position of extremum of the triplet yield dependence on external magnetic field will correlate with the value of the average electron exchange coupling in the radical ion pair ($H_{\max} \sim 2J_0$). The majority of experimentally observed values of J_0 are in the range of up to 1 T [12, 14, 25, 26]. The values of HFI constants and the difference of g-factors [27, 28] of the donor and acceptor fragments in discussed biradical ion let us also expect the appearance of MFE formed via the HFI and relaxation mechanisms [29].

To imagine the possible spatial configurations of the dyads and a possible variation of the distance between the donor and acceptor groups, which will determine the energy of the electron exchange interaction in the biradical ion, we have examined the calculated energy variation with the torsion angle of CH_3–C–C=O bond of (*R,S*)- and (*S,S*)-NPX-Pyr (Fig. 1). These figures show that the distances between the donor and acceptor groups of the dyads in the minima of energy differ significantly for (*R,S*)- and (*S,S*)-enantiomers.

In this case, the minimum distance between the donor and acceptor groups (the nitrogen atom and the center of the naproxen ring) is around 0.5–0.55 nm, and the maximum distance is about 0.8–0.9 nm. On the other hand, it is well known that biradicals of cyclic ketones having the chain length of 10 carbon atoms have maximum of CIDNP in magnetic field around 100 mT. It could be expected that the maximum of MFE in the system under study will be in magnetic field less than that one because of the more rigid expected structure of the biradical ion of the dyad. Taking into account all these considerations, magnetic field strength in this investigation was varied from 0 to 70 mT.

MFE on the yield of triplet state of the dyad was measured using laser flash photolysis. An example of the triplet decay kinetic for NPX-Pyr is shown in Fig. 2. Magnetic field dependence of the triplet yield was measured at the maximum of these curves. Unfortunately, no observable MFE was detected in this system (Fig. 3).

The reason for the absence of the observable MFE might be the wrong choice of the range of magnetic fields. This is possible if the energy of electron exchange interaction in the biradical ion is much higher in comparison with the value of the

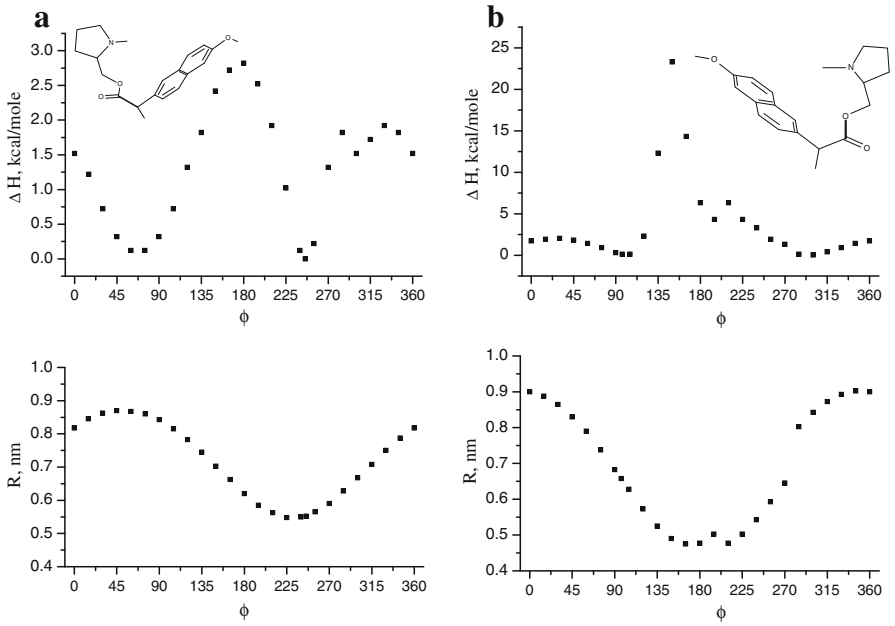

Fig. 1 Calculated changes in the heat of formation and the distance between the donor and acceptor groups of **a** (*R,S*)-NPX-Pyr and **b** (*S,S*)-NPX-Pyr as a function of the torsion angle (ϕ) of CH_3–C–C=O bond

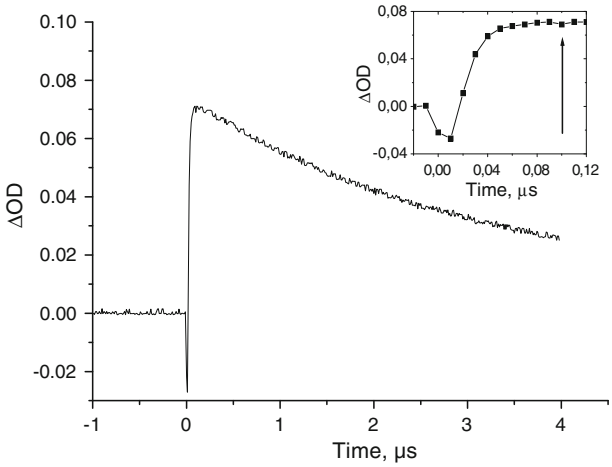

Fig. 2 Kinetics of transient absorption of (*R,S*)-NPX-Pyr triplet state detected after laser pulse ($\lambda_{obs} = 440$ nm). *Inset* shows the initial part of the kinetics. *Arrow* indicates time delay for monitoring of MFE

applied external magnetic field. According to our calculations [30], in a radical pair with $J \gg A$ (HFI constant) the absence of MFE formed through the HFI mechanism is also possible. On the other hand, the very rapid growth of the triplet yield, with

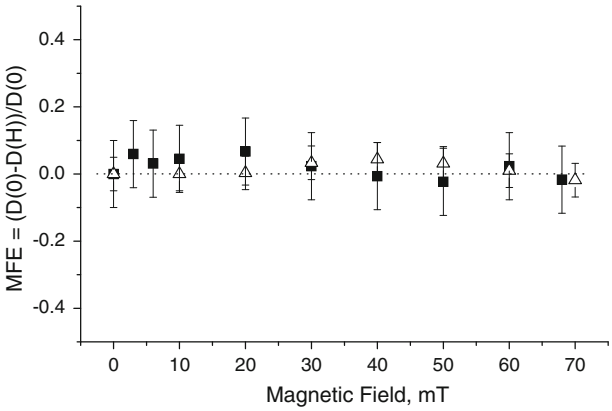

Fig. 3 Magnetic field dependence of the yield of (*R,S*)-NPX-Pyr triplet state in acetonitrile (*filled square*) and tetrahydrofuran (*open triangle*), measured by laser flash photolysis

the characteristic time of about 20 ns (see inset in Fig. 2), makes us doubt that the PET stage is the main route of the triplet state formation. Note that both the PET and the exciplex formation are typical photoinduced processes, which can be expected to occur between excited naphthalene chromophores and electron donors like amines [15]. These two pathways should be considered as the main quenching mechanisms. The formation of the trace amounts of exciplex during ultraviolet (UV) irradiation of the dyads in acetonitrile was described earlier [16]. The calculations show that the exciplex formation is favored in nonpolar and weakly polar solvents, while in polar media PET has to dominate (Fig. 4). These calculations were performed using the Rehm–Weller equation $\Delta G(\varepsilon) = [E_{ox}(D/D^{+}) - E_{red}(A^{-}/A)]_{\varepsilon 0} - e/\varepsilon a + \Delta G_{solv} - E_{0\text{–}0}\,(^{1}D^{*})$. Here $\Delta G_{solv} = e^{2}/2(1/R^{D+} + 1/R^{A-}) \times (1/\varepsilon - 1/\varepsilon_{0})$, ε_0 is the dielectric constant of the solvent, in which redox potentials were determined. R^{D+}, R^{A-} and a are the radii of the radical cation, radical anion, and the distance between them, respectively. E_{ox}(N-methylpyrrolidine) = 1.0 V versus saturated calomel electrode (SCE), E_{red}(2-methoxynaphtalene) = −2.6 V versus SCE were determined in acetonitrile [31], and $E_{0\text{–}0}$(NPX) = 3.69 eV.

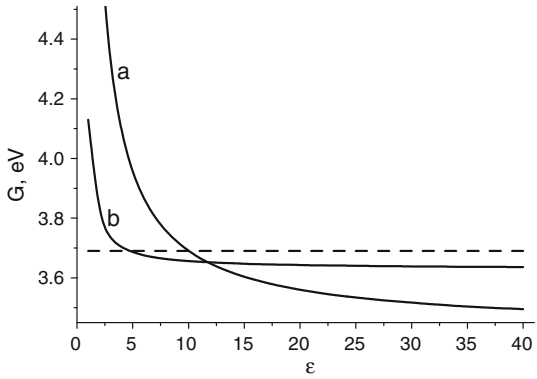

Fig. 4 Dependences of the free energy of NPX-Pyr biradical ion (**a**) and exciplex (**b**) on dielectric constant of the solvent (ε). *Dashed line* shows the energy of an excited singlet state of NPX-Pyr

To verify the participation of the PET stage in the quenching of the NPX-Pyr excited state we use another spin chemistry method—high-field CIDNP. Figure 5 shows NMR and CIDNP spectra of (*S,S*)-NPX-Pyr in acetonitrile. The (*R,S*)-enantiomer demonstrates identical CIDNP pattern. Noticeable polarization was detected only for pyrrolidine protons in α-position to N atom. It is reasonable to suggest that this polarization is derived from the biradical ion, because HFI constants of amine radical cation are maximal on the N–CH_3, N–CH_2 and N–CH groups in the system under study [32].

It is reasonable to suggest that this polarization is formed through the S–T_0 mechanism in accordance with the results of numerous previous investigations of chemical polarization formed in short biradicals in high magnetic field during the photolysis of cyclic ketones [11] and benzoquinone in the presence of quadricyclane [33]. In the framework of the S–T_0 mechanism, the appearance of chemical polarization of the NPX–Pyr dyad would be possible if there is some other channel of nuclear polarization decay in addition to back electron transfer in the biradical ion. It is reasonable to suggest that in the system under study the polarization might decay due to the one of the following processes: chemical reaction, fast relaxation in the biradical or the relaxation of back electron transfer product—long-lived triplet state.

Since the indicative feature of CIDNP formed in radical ion pairs is their high sensitivity to the solvent polarity, the dependence of chemical polarization of N-methylpyrrolidine protons on dielectric constant of the solvent (ε) has been investigated to clarify the role of the PET channel in the quenching of excited state of the NPX–Pyr dyad. Note that CIDNP effects observed for this dyad have to be a superposition of several contributions, namely, the contributions from the recombination of S and T states of the biradical ion (intramolecular back electron transfer), from the bimolecular quenching of the excited state of the chromophore of the dyad by another dyad in the ground state, as well as the contribution from bulk

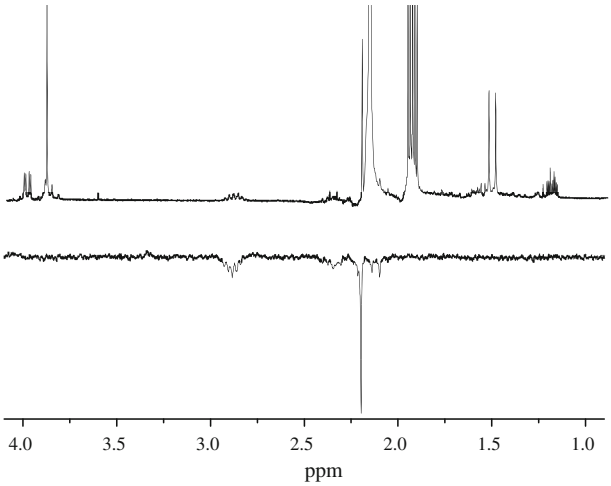

Fig. 5 NMR (*top*) and TR CIDNP at 1 μs delay (*bottom*) spectra detected after laser irradiation of (*S,S*)-NPX-Pyr (1 mM) in CD_3CN

processes (degenerate electron exchange of the radical ions with neutral molecules and F-pairs). To minimize the contribution from intermolecular processes to the observed CIDNP, low concentration of the dyad ($\leq$1 mM) was used in our experiments. TEA was added as an additional external quencher of the excited state of the naproxen fragment. In this case, the rate of intramolecular quenching of the excited singlet state of the dyad would significantly exceed the rates of intermolecular processes: $W_{\text{intra}} = 1.8 \times 10^8\ \text{s}^{-1}$ and $2.8 \times 10^8\ \text{s}^{-1}$, for (*S*,*S*)- and (*R*,*S*)-NPX-Pyr, respectively; $W_{\text{TEA}} = 5 \times 10^9 \times$ [TEA] $= 5 \times 10^7\ \text{s}^{-1}$ and $W_{\text{inter}} = 5 \times 10^9 \times$ [dyad] $= 5 \times 10^6\ \text{s}^{-1}$, for the used experimental concentrations and assuming that the rate constants of the quenching of the excited state of the dyad by the dyad itself and by amine are equal [15]. Thus, we suppose that all experimental dependences of NPX dyad CIDNP that will be described later refer to intramolecular PET.

Experimental dependences of the TR CIDNP intensity for N-methylpyrrolidine protons (N-CH_3 and N-CH) and N-CH_2 protons of TEA on solvent dielectric constant (ε) are shown in Fig. 6. Dependences of the CIDNP intensities for CH_2 protons of TEA and N–CH_3 protons of N-methylpyrrolidine on solvent polarity in the systems DMN + TEA, Me-NPX + TEA and Me-NPX + Ac-Pyr are shown in Figs. 7 and 8. All these systems have very close values of redox potentials in acetonitrile: $E_{\text{red}} = 2.60$ V versus SCE for methoxy-naphthalene; $E_{\text{red}} = 2.58$ V versus SCE for DMN; $E_{\text{ox}} = 0.96$ V versus SCE for TEA and $E_{\text{ox}} = 1.0$ V versus SCE for N-methylpyrrolidine [31].

Note that dependences of the CIDNP effects for protons of the N–methylpyrrolidine fragment and TEA detected during UV irradiation of NPX–Pyr dyad differ significantly from the profiles detected in photoinduced interaction of Ac-Pyr and TEA with naphthalene derivatives. In particular, at high solvent polarity, the sign of CIDNP for Ac-Pyr (Fig. 8b) or TEA (Figs. 6b, 7, 8a) is opposite to that for protons of the N-methylpyrrolidine fragment of the dyad (Fig. 6). Moreover, at low polarity, $\varepsilon < 10$, CIDNP effects were observed only in the photolysis of NPX–Pyr dyad (Fig. 6) and Me-NPX + Ac-Pyr system (Fig. 8b).

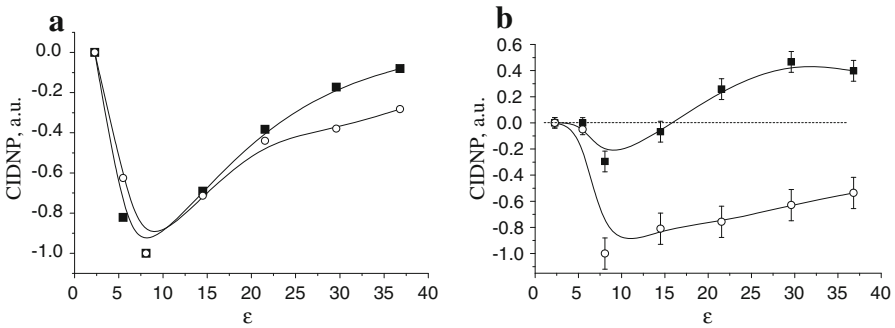

Fig. 6 Dependences of the TR CIDNP (delay 1 μs) intensity for N–CH_3 protons of NPX-Pyr dyad (1 mM) on solvent polarity in the absence (**a**, *left*: *filled square* (*R*,*S*)- and *open circle* (*S*,*S*)-dyad) and in the presence of TEA (10 mM) (**b**, *right*: *open circle* (*R*,*S*)-dyad and *filled square* N–CH_2 protons of TEA)

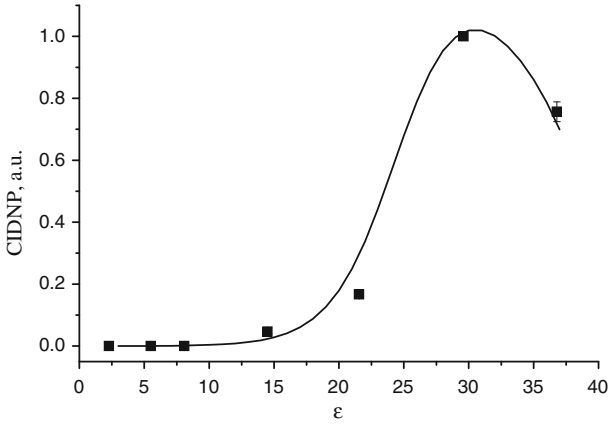

Fig. 7 Dependence of the TR CIDNP (delay 1 μs) intensity for N–CH_2 protons of TEA on solvent polarity in its photoreaction with DMN

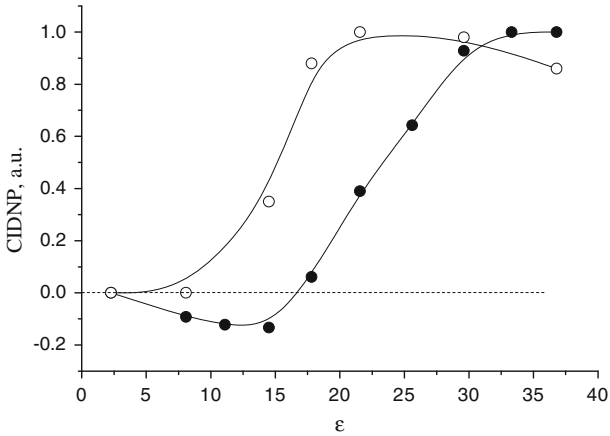

Fig. 8 Dependences of the TR CIDNP (delay 1 μs) intensity on solvent polarity in the systems: Me-NPX and TEA (*open circle*); Me-NPX and Ac-Pyr (*filled circle*)

Furthermore, the dependences for N–CH_2 protons of TEA detected in photoinduced interaction of TEA with the dyad (Fig. 6b) and N–CH_3 protons of Ac-Pyr in its interaction with Me-NPX show the alternation of the signs of CIDNP (Fig. 8).

To explain the unusual CIDNP dependences on solvent polarity, we turned to reference data. According to the classical considerations, the S-type curve is the typical shape of the dependence of the quantum yields of solvent separated RIP on solvent dielectric constant [34]. It is also known that charge transfer complexes, for instance, the complex of stilbene with fumaronitrile, under UV irradiation form radical cations of stilbene even in solvents with low polarity, bromobenzene and dimethoxyethane [35]. The authors suggested that the presence of the radical cation

in nonpolar solvents is due to fast, comparable with lifetime of RIP, transitions between solvent separated and contact RIP (exciplex). The observation of MFE on exciplex fluorescence in chain-linked phenanthrene–dimethylaniline dyad and in supramolecular complex of zinc(II)–tetraphenylporphyrin with viologen, which was described by Cao et al. [36], was also explained by the existence of fast equilibrium between RIP and exciplex.

Because the CIDNP intensity in the systems under study in different solvents is mostly determined by RIP concentration, for radical ions which have redox potentials close to the values for NPX and Pyr significant effects should appear at polarity around $\varepsilon = 15$–20. Examples are CIDNP effects for TEA protons in systems DMN + TEA and Me-NPX + TEA detected in solvents with different polarity (Figs. 7, 8). Equal CIDNP signs for these protons point to the same predominant channel of RIP recombination in both systems. Note that T-RIP recombination is the main channel of the photoinduced interaction of naphthalene with TEA in polar solvents, as was established earlier [32]. Spin-dependent recombination probability for a radical ion pair where both singlet and triplet states being reactive was considered earlier using Green function theory [37]

$$w_S = \frac{k_S\tau_S + k_s k_T(2\tau_S - \tau)\tau}{1 + (k_S + k_T)\tau_S + k_s k_T(2\tau_S - \tau)\tau},$$
$$w_T = \frac{k_T(\tau - \tau_S)}{1 + (k_S + k_T)\tau_S + k_s k_T(2\tau_S - \tau)\tau}$$

where k_S and k_T are recombination rate constants, τ is the residence time of radicals in the reaction zone, and τ_S is the residence time of radicals in the reaction zone only in the singlet state.

The sign of the geminal CIDNP that is formed in RIP is determined by the ratio $\frac{\lambda_S}{\lambda_T}$ of parameters, which characterized recombination of RIP, where ($\lambda_S = \frac{k_S\tau}{1+k_S\tau}$) and ($\lambda_T = \frac{k_T\tau}{1+k_T\tau}$) [38]. Thus, $\lambda_T > \lambda_S$ holds for the abovementioned interaction of DMN and Me-NPX with TEA. The participation of Ac-Pyr, instead of TEA, in reaction with Me-NPX changes dramatically the shape of the CIDNP dependence on polarity (Fig. 8). Thus, the triplet recombination channel plays the dominant role in the solvents with high polarity ($\varepsilon > 20$). A decrease of polarity down to $\varepsilon = 15$ reduces CIDNP intensity, and further decreasing of the dielectric constant leads to the change of sign of CIDNP for N–CH_3 protons. The change of sign most probably means that in this case λ_S becomes larger than λ_T. This should be expected if S state of RIP converts into exciplex. Analysis of CIDNP for protons of the pyrrolidine fragment of the dyad shows that $\lambda_T < \lambda_S$ in the entire polarity range. If this results from singlet exciplex formation, further decrease of CIDNP intensity with the increase of polarity (Fig. 6) might be explained by the change of the ratio of λ_S and λ_T arising from the increase of the triplet channel recombination in polar media. Additional evidence for the formation of exciplex of the NPX-Pyr dyad is provided by the profile of the CIDNP dependence on polarity measured in the photoinduced reaction of the NPX-Pyr dyad with TEA. While CIDNP for methyl protons of the pyrrolidine fragment is identical to that detected in the absence of TEA and corresponds to intramolecular PET, CIDNP effects for N–CH_2 protons of TEA, which are polarized through intermolecular quenching process, demonstrate the

abovementioned peculiarities (Fig. 6b). A comparison of the polarity dependences of CIDNP for TEA protons detected in quenching of the excited state of the NPX-Pyr dyad and Me-NPX itself by TEA (Figs. 6b, 8) points to the participation of the exciplex of the dyad in the reaction with TEA. Because the same paramagnetic species are formed in both reactions, the reason for the appearance of CIDNP in solvents with low polarity ($5 < \varepsilon < 15$) and the change of the dominant recombination channel in high polarity ($\lambda_T < \lambda_S$) most probably might be connected with the singlet exciplex formation. Possible ways for quenching of the excited singlet state of the NPX-Pyr dyad in the presence and in the absence of TEA are shown below.

These schemes reflect the main peculiarity of the system under study connected with the existence of fast, comparable with the time of spin evolution (K_{S-T}), equilibrium between the exciplex and the biradical ion (K_{exp}) or RIP that are formed in the presence of TEA (k_{exp} and k_{ee}). To explain the appearance of CIDNP for TEA protons in weakly polar media ($\varepsilon < 10$), the step of electron transfer from the pyrrolidine fragment of the dyad to TEA has been included in Scheme 2. Since the difference of oxidation potentials of TEA and the pyrrolidine fragment of the dyad is less than 0.05 V, it is reasonable to expect rapid electron exchange between the radical cation of TEA and the pyrrolidine fragment of the dyad (k_{ee} in Scheme 2). Due to charge separation in the biradical ion of the dyad, the electron exchange should lead to formation of the initial charge-separated RIP of the radical anion of the dyad and the radical cation of TEA ($^{-}$NPX-Pyr TEA^{+}). It is this initial charge separation in RIP that is the origin of the CIDNP effects for TEA protons in solvents with low polarity.

According to these schemes, the signs of the observed CIDNP are determined by the ratios of recombination constants k_S, k_T and k_{exp}. Correspondingly, the recombination probabilities for S and T spin states of RIP are given by the following equations: $\lambda_T = \frac{k_T\tau}{1+k_T\tau}$, $\lambda_S = \frac{(k_S+k_{exp})\tau}{1+(k_S+k_{exp})\tau}$.

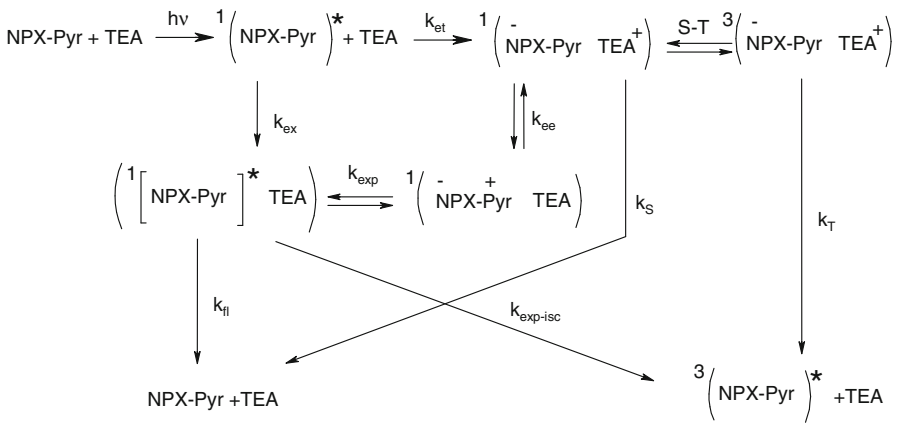

Scheme 2 Quenching of the excited singlet state of the NPX-Pyr dyad in solution in the presence of TEA

Analysis of energy diagrams for the photoinduced processes in the NPX-Pyr dyad in the presence of TEA in the media of different polarity leads to the conclusion that the change of the CIDNP sign for TEA is possible under the following conditions (Fig. 9).

According to Fig. 9, the ratios of k_{exp}, k_S and k_T in media of different polarity depend on the free energy changes ΔG_3, ΔG_1 and ΔG_2, correspondingly. One can expect that at low polarity ($\varepsilon < 20$) ΔG_1, ΔG_2, $\Delta G_3 < 0$ an $|\Delta G_3| < |\Delta G_2| < |\Delta G_1|$. In this case, the expected ordering of the rate constants will be $k_{exp} > k_T > k_S$, and the sign of CIDNP for the TEA protons corresponds to back electron transfer from S-RIP ($\lambda_S > \lambda_T$). On the other hand, at higher polarity ($\varepsilon > 20$) one can expect that ΔG_1, $\Delta G_2 < 0$ and $\Delta G_3 > 0$ and $|\Delta G_2| < |\Delta G_1|$. Then $k_T > k_S > k_{exp}$, and the sign of CIDNP for the TEA protons will correspond to $\lambda_T > \lambda_S$. Thus, the observed CIDNP effects and their dependence on solvent polarity can be explained only by including exciplex (existing in equilibrium with RIP, $K_{exp} \sim K_{S-T}$) into the reaction scheme.

Thus, analysis of the dependences of CIDNP intensity on solvent polarity points to the participation of singlet exciplex in quenching of the NPX excited state in the following three systems: NPX-Pyr dyad in the presence and in the absence of TEA, and Me-NPX in the presence of Ac-Pyr. Reference data are also available on the detection of exciplex of NPX with N-methylpyrrolidine by optical methods [15]. CIDNP polarity dependences for these systems manifest both a similarity, the existence of a region where $\lambda_S > \lambda_T$, and a difference, in the region of high polarity. So, CIDNP analysis shows the domination of the singlet recombination channel up to solvent dielectric constant $\varepsilon = 20$ in the case of quenching of the excited states of Me-NPX in solution, whereas for the process of quenching of the excited state of the NPX-Pyr dyad $\lambda_S > \lambda_T$ in the entire range of solvent polarity. The latter means that dyad quenching through the exciplex competes with PET even in polar solvents.

Taking into account the significance of latter conclusion, we made an attempt to consider theoretically possible reasons of the difference between the profiles of curves from Fig. 10.

Another peculiarity of spin and molecular dynamics in linked system is demonstrated in Fig. 10. As mentioned above, all energetic characteristics and MR parameters of the systems from Fig. 10 are identical. Consequently, one can expect the same set of recombination rate constants for these systems. Then, the main difference between dependences of CIDNP on solvent polarity in the dyad and in

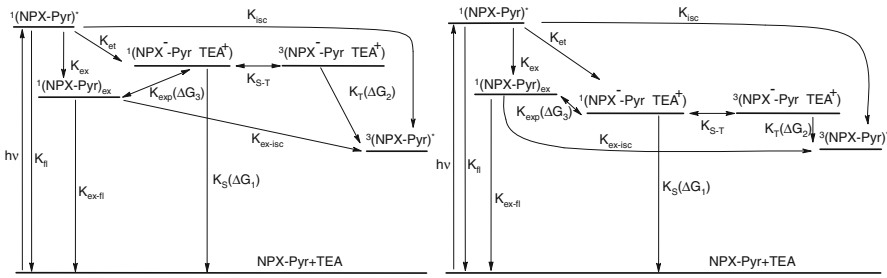

Fig. 9 Energy diagrams for the photoinduced processes in the NPX-Pyr dyad in the presence of TEA: *left* low polarity, *right* high polarity

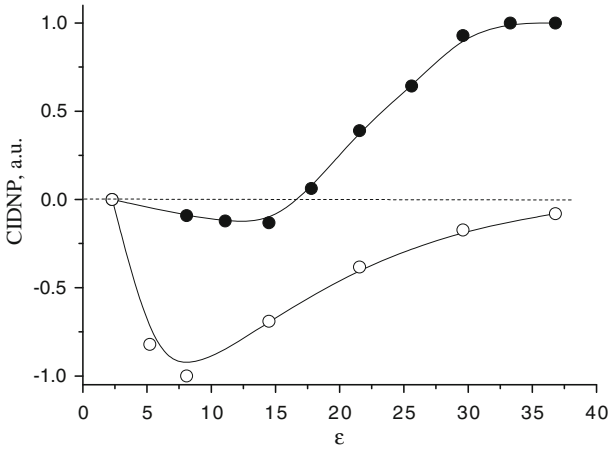

Fig. 10 Dependences of CIDNP for the pyrrolidine fragment on solvent polarity: for (*R,S*)-NPX-Pyr from Fig. 6a (*open circle*), and Me-NPX + Ac-Pyr system from Fig. 8 (*filled circle*)

the encountering partners in the solution might be connected with the bigger contribution of conformation with short distance between the donor and acceptor in the dyad. Then, the prevailing of singlet recombination in all range of polarity that leads to the appearance of negative polarization might result from fast nuclear relaxation of pyrrolidine protons of dyad's triplet.

Taking into account the absence of any significant external magnetic field influence on triplet yield in the NPX-Pyr dyad, we can suggest that the main reason for this is that one channel of triplet formation is internal intersystem conversion of exciplex ($k_{exp\text{-}isc}$). The process of the dyad triplet state formation via exciplex is shown in Scheme 3 and the energy diagram (Fig. 9). According to Scheme 3, the absence of MFE will result from the compensation of the effects with opposite signs arising from the recombination of T and S states of the biradical ion. Note that examples of small MFEs detected in systems that involve exciplex, in which high internal intersystem conversion takes place, have been described in literature. Thus, reference data are available about molecular dynamics and MFEs detected by T–T absorption or luminescence in the processes of quenching of the excited states of aromatic hydrocarbons by aromatic amines [39–42]. The analysis showed that the range of MFEs in such systems first of all is determined by the efficiency of the internal S–T conversion in exciplex from which RIP was produced. Indeed, there are very weak MFEs (2–4%) on T–T absorption of anthracene detected by quenching of its excited state by dimethylaniline. At the same time, high internal intersystem conversion in "anthracene–dimethylaniline" exciplex was established by Mataga [42].

Thus, the investigation of the elementary mechanism of quenching of chromophore excited state in the NPX-Pyr dyad and in related systems by means of spin chemistry methods points to the following peculiarities detected in the linked system. First of all, it is the involvement of singlet exciplex of the dyad along with the intramolecular PET in quenching processes. Another characteristic feature is

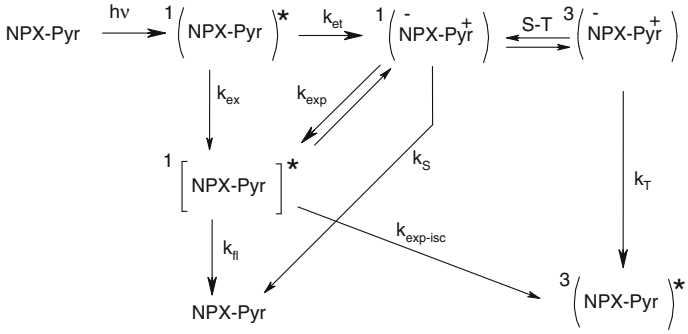

Scheme 3 Quenching of the excited singlet state of the NPX-Pyr dyad in solution

connected with long lifetime of the biradical ion in comparison with the lifetime of RIP formed by the diffusion quenching processes.

As for the nature of the abovementioned influence of chiral centers on chemical reactivity of NPX-Pyr dyads, spin chemistry study allows us to make some suggestions. At first, we were under the impression that the most plausible reason of the difference between the rates of quenching of the excitation of the chromophore of the (*R,S*)- and (*S,S*)-NPX-Pyr dyads could be the difference of the energy of electron exchange interaction in the biradical ions of (*R,S*)- and (*S,S*)-enantiomers. In this case, the stereo selectivity might be the result of different rates of back electron transfer in biradical ions of the isomers. The way of the possible influence of back electron transfer rates on fluorescence quenching, connected with existence of equilibrium between the exciplex and the biradical ion, is shown in Scheme 3. However, the small intensity of CIDNP for the dyads detected in solvents with high polarity, the identity of the CIDNP effects for the enantiomers, and the absence of the influence of external magnetic field on the triplet yield of the dyads make us conclude that processes in the biradical ions are not the main source of the stereo selectivity. Then it might be reasonable to consider the possibility of processes in the exciplex of the dyads to influence the rate of fluorescence quenching. The abovementioned internal singlet–triplet conversion of exciplex has to be highly sensitive to both energetic and steric effects [43].

It is believed that future investigations of the source of the influence of chiral centers on photochemistry of linked systems have to involve the study of processes both in the biradical ion and in the exciplex.

Acknowledgments This work was supported by the grants 08-03-00372 and 11-03-01104 of the Russian Foundation for Basic Research, and the grant of Priority Programs of the Russian Academy of Sciences, nr. 5.1.5.

References

1. J.S. Park, E. Karnas, K. Ohkubo, P. Chen, K.M. Kadish, S. Fukuzumi, C.W. Bielawski, T.W. Hudnall, V.M. Lynch, J.L. Sessler, Science **329**, 1324–1327 (2010)
2. S.Y. Reece, D.G. Nocera, Annu. Rev. Biochem. **78**, 673–699 (2009)

3. M.S. Afanasyeva, M.B. Taraban, P.A. Purtov, T.V. Leshina, C.B. Grissom, J. Am. Chem. Soc. **128**, 8651–8658 (2006)
4. M.A. Fox, M. Chanon, in *Photoinduced Electron Transfer. C: Photoinduced Electron Transfer Reactions: Organic Substrates* (Elsevier, New York, 1988), p. 754
5. P.J. Hayball, R.L. Nation, F. Bochner, Chirality **4**, 484–487 (1992)
6. N. Suesa, M.F. Fernandez, M. Gutierrez, M.J. Rufat, E. Rotllan, L. Calvo, D. Mauleon, G. Carganico, Chirality **5**, 589–595 (1993)
7. A.M. Evans, J. Clin. Pharmacol. **36**, 7–15 (1996)
8. Y. Inoue, T. Wada, S. Asaoka, H. Sato, J.-P. Pete, Chem Commun. **4**, 251–259 (2000)
9. T. Yorozu, K. Hayashi, M. Irie, J. Am. Chem. Soc. **103**, 5480–5548 (1981)
10. N.J. Turro, in *Modern Molecular Photochemistry* (Benjamin/Cummings, San Francisco, 1978)
11. K.M. Salikhov, Y.N. Molin, R.Z. Sagdeev, A.L. Buchachenko, in *Spin Polarization and Magnetic Field Effects in Radical Reactions* (Akademiai Kiado, Budapest, 1984), p. 419
12. E.A. Weiss, M.A. Ratner, M.R. Wasielewski, J. Phys. Chem. A **107**, 3639–3647 (2003)
13. A.S. Lukas, P.J. Bushard, E.A. Weiss, M.R. Wasielewski, J. Am. Chem. Soc. **125**, 3921–3930 (2003)
14. R. Nakagaki, K. Mutai, M. Hiramatsu, H. Tukada, S. Nakakura, Can. J. Chem. **66**, 1989–1996 (1988)
15. M.C. Jim′enez, U. Pischel, M.A. Miranda, J. Photochem. Photobiol. C Photochem. Rev. **8**, 128–142 (2007)
16. S. Abad, U. Pischel, M.A. Miranda, Photochem. Photobiol. Sci. **4**, 69–74 (2005)
17. U. Pischel, S. Abad, L.R. Domingo, F. Bosca, M.A. Miranda, Angew. Chem. Int. Ed. **42**, 2531–2534 (2003)
18. G.L. Closs, R.J. Miller, J. Am. Chem. Soc. **101**, 1639–1641 (1979)
19. G.L. Closs, R.J. Miller, J. Am. Chem. Soc. **103**, 3586–3588 (1981)
20. M. Goez, Chem. Phys. Lett. **188**, 451–456 (1992)
21. I.F. Molokov, Y.P. Tsentalovich, A.V. Yurkovskaya, R.Z. Sagdeev, J. Photochem. Photobiol. A **110**, 159–165 (1997)
22. U. Pischel, S. Abad, M.A. Miranda, Chem. Commun. **9**, 1088–1089 (2003)
23. H. Hayashi, S. Nagakura, Bull. Chem. Soc. Jpn. **57**, 322–328 (1984)
24. Y. Sakaguchi, H. Hayashi, S. Nagakura, Bull. Chem. Soc. Jpn. **53**, 39–42 (1980)
25. H. Yonemura, H. Nakamura, T. Matsuo, Chem. Phys. Lett. **155**, 157–161 (1989)
26. N. Hata, M. Hokawa, Chem. Lett. **10**, 507–510 (1981)
27. M. Shiotani, L. Sjoeqvist, A. Lund, S. Lunell, L. Eriksson, M.B. Huang, J. Phys. Chem. **94**, 8081–8090 (1990)
28. E. Schaffner, H. Fischer, J. Phys. Chem. **100**, 1657–1665 (1996)
29. Y. Mori, Y. Sakaguchi, H. Hayashi, Chem. Phys. Lett. **286**, 446–451 (1998)
30. I.M. Magin, A.I. Kruppa, P.A. Purtov, Chem. Phys. **365**, 80–84 (2009)
31. K.K. Barnes, *Electrochemical Reactions in Nonaqueous Systems* (M. Dekker, New York, 1970), p. 560
32. J. Bargon, J. Am. Chem. Soc. **99**, 8350–8351 (1977)
33. M. Goez, I. Frisch, J. Phys. Chem. A **106**, 8079–8084 (2002)
34. A.K. Chibisov, Russ. Chem. Rev. **50**, 615–629 (1981)
35. J. Goodman, K. Peters, J. Am. Chem. Soc. **107**, 1441–1442 (1985)
36. H. Cao, Y. Fujiwara, T. Haino, Y. Fukazawa, C.-H. Tung, Y. Tanimoto, Bull. Chem. Soc. Jpn. **69**, 2801–2813 (1996)
37. P.A. Purtov, A.B. Doktorov, Chem. Phys. **178**, 47–65 (1993)
38. A.I. Kruppa, O.I. Mikhailovskaya, T.V. Leshina, Chem. Phys. Lett. **147**, 65–71 (1988)
39. M.E. Michel-Beyerle, R. Haberkorn, W. Bube, E. Steffens, H. Schröder, H.J. Neusser, E.W. Schlag, H. Seidlitz, Chem. Phys. **17**, 139–145 (1976)
40. K. Schulten, H. Staerk, A. Weller, H.-J. Werner, B. Nickel, Z. Phys. Chem. **101**, 371–390 (1976)
41. K. Gnadig, K.B. Eisenthal, Chem. Phys. Lett. **46**, 339–342 (1977)
42. T. Nishimura, N. Nakashima, N. Mataga, Chem. Phys. Lett. **46**, 334–338 (1977)
43. M.G. Kuzmin, I.V. Soboleva, E.V. Dolotova, D.N. Dogadkin, High Eng. Chem. **39**, 86–96 (2005)